



Ratiometric SERS detection of polycyclic aromatic hydrocarbons assisted by β -cyclodextrin-modified gold nanoparticles

Zhao Yu¹ · Michael F. Grasso¹ · Hanna H. Sorensen¹ · Peng Zhang¹

Received: 23 January 2019 / Accepted: 16 May 2019 / Published online: 31 May 2019
© Springer-Verlag GmbH Austria, part of Springer Nature 2019

Abstract

A surface-enhanced Raman scattering (SERS) method is described for the determination of trace polycyclic aromatic hydrocarbons (PAHs) in the environment efficiently and economically. Detection sensitivity is improved by modifying gold nanoparticles (AuNPs) with 4-mercaptophenylboronic acid (4-MPBA) conjugated to β -cyclodextrin (β -CD) as a new method for ratiometric determination of PAHs in solution. Pyrene (with a Raman band at 580 cm^{-1}) and anthracene (750 cm^{-1}) were used as the model analytes, while 4-MPBA (1570 cm^{-1}) was used as the internal reference to normalize the SERS signals. The intensity ratios of pyrene/4-MPBA increase linearly in the 2 to 10 nM pyrene concentration range, and the intensity ratios of anthracene/4-MPBA increase linearly in the 10 to 100 nM anthracene concentration range. The detection limits are 0.4 nM for pyrene and 4.4 nM for anthracene. This method was applied to the determination of the two analytes in soil sample extracts and the recoveries of pyrene (at levels of $236\text{ ng}\cdot\text{g}^{-1}$ and $170\text{ ng}\cdot\text{g}^{-1}$) and anthracene ($334\text{ ng}\cdot\text{g}^{-1}$ and $510\text{ ng}\cdot\text{g}^{-1}$) agreed well with the results from GC-MS analyses. The good recovery rates (101.8% and 102.5% for pyrene and 106.4% and 101.7% for anthracene) confirmed the reliability of the method.

Keywords Solution SERS · β -Cyclodextrin modification · Internal reference · Pyrene · Anthracene · Soil samples

Introduction

Polycyclic aromatic hydrocarbons (PAHs) are a group of common, persistent organic pollutants with two or more condensed aromatic rings, which are mainly formed as products from the incomplete combustion of fuels [1, 2]. PAHs can be found in soil, water and air, which may be absorbed by plants and animals, and become health hazards to humans due to the potential carcinogenicity [3–6]. Current standard methods such as gas chromatography in combination with mass spectrometry (GC-MS) [7, 8], gas chromatography (GC) [9], and high performance liquid chromatography with fluorescence detection (HPLC/FLD) [10, 11] are used to

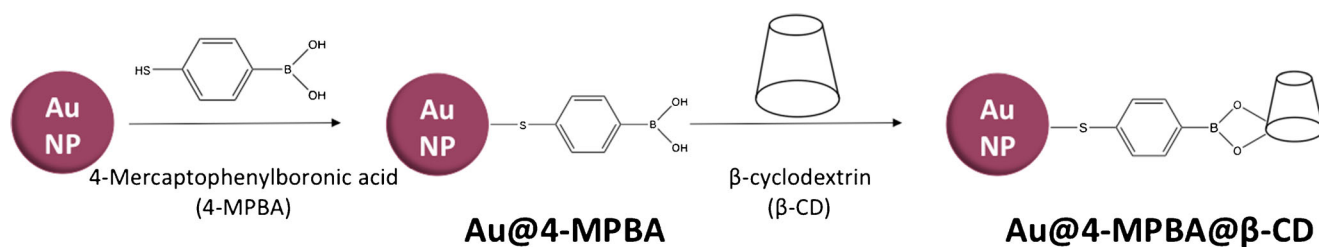
detect PAHs in environmental and food samples. These methods usually require complicated sample preparations and sophisticated instruments, which increase the time and expense for the analyses [12].

Surface enhanced Raman scattering (SERS) has emerged as an alternative method to detect environmental pollutants due to the enhancement of analytes' Raman peaks induced by the localized surface plasmon on the rough surface of SERS substrates [13, 14]. Sample preparation for SERS measurements is simple, and the measurements are relatively quick compared to chromatography. Therefore, SERS measurements have become more common in environmental analyses [15–19]. In the literature, there has been a report on using thiol-modified, silver-coated magnetic nanoparticles (MNPs) as SERS substrate to identify and detect PAHs [20]. Silver shell on the MNPs provided the localized surface plasmon under laser excitation for SERS signal enhancement, and pentanethiol improved the surface polarity to attract PAHs in aqueous solution to the nanoparticles. SERS measurements were done after the nanoparticles were collected by a magnet and dried on a silica wafer, and the calculated detection limit was at $\mu\text{g}\cdot\text{L}^{-1}$ level. Another report described the use of a β -cyclodextrin (β -CD) modified silica-polymer brush (Si-PGMA) and β -CD-SH modified gold

Electronic supplementary material The online version of this article (<https://doi.org/10.1007/s00604-019-3511-9>) contains supplementary material, which is available to authorized users.

✉ Peng Zhang
peng.zhang@uc.edu

¹ Department of Chemistry, University of Cincinnati, Cincinnati, OH 45221, USA



nanoparticles (AuNPs) with Rh6G to form a sandwich structure in the presence of PAHs [21]. SERS measurements were done after washing the silica-polymer brush, and the signal intensity of Rh6G indicated the concentration of PAHs indirectly with the detection limit at the nM level. These reports focused on the measurement of analytes on solid SERS substrates, which requires time to prepare the dried samples and tends to have large fluctuations in the SERS signals when the concentration of the analyte is low.

Herein we report an effective and sensitive SERS method to detect PAHs in homogenous solutions assisted by β -CD modified AuNPs as the SERS substrate. β -CD was used to capture the PAHs and bring the analytes close to the AuNPs surface. 4-Mercaptophenylboronic acid (4-MPBA) was used not only to conjugate β -CD to the surface of AuNPs, but also to act as an internal reference to improve the reliability of the SERS measurement [22, 23]. In this study, pyrene and anthracene were

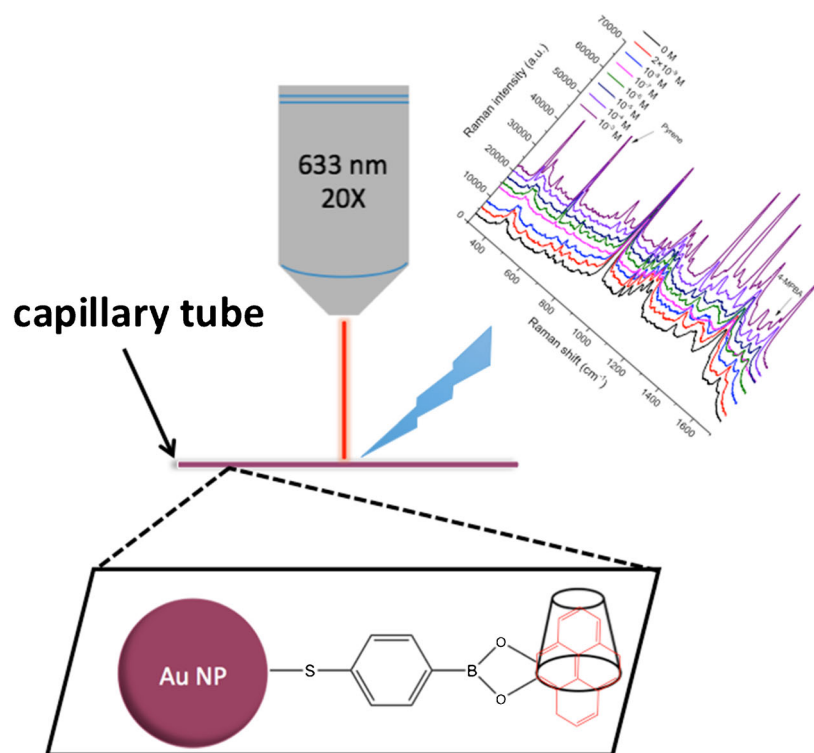
used as the model PAHs for detection and linear relationships were established between the SERS intensity ratio of PAH/4-MPBA and PAH concentration. This method was applied to measure PAHs in soil samples, and the recoveries of the analytes were very close to the results from GC-MS.

Material and methods

Chemicals and materials

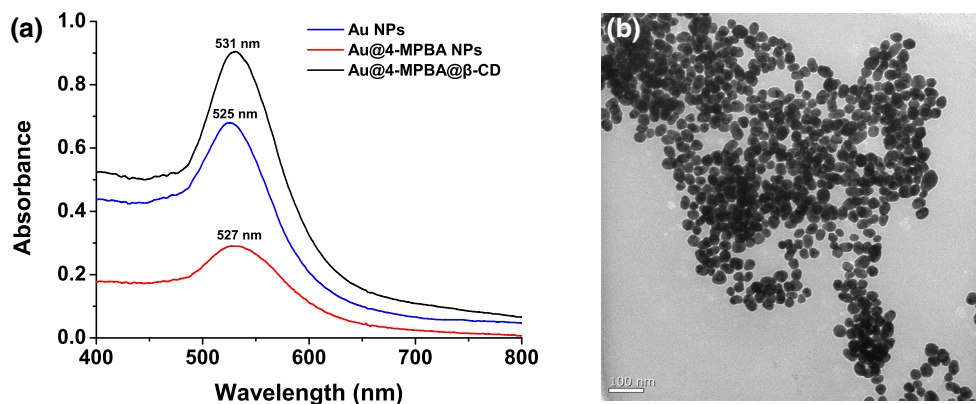
Gold(III) chloride trihydrate ($\text{HAuCl}_4 \cdot 3\text{H}_2\text{O}$), sodium citrate, 4-Mercaptophenylboronic acid (4-MPBA), β -Cyclodextrin (β -CD), pyrene, and anthracene were purchased from Sigma-Aldrich (St. Louis, MO, www.sigmaaldrich.com). Acetone and ethanol were purchased from Fisher Scientific (Hampton, NH, www.fishersci.com). Deionized (DI) water

Scheme 2 Raman measurements of Au@4-MPBA@ β -CD NPs mixed with pyrene solutions in capillary tube illustration



Au@4-MPBA@ β -CD solution mixed with pyrene

Fig. 1 **a** UV-vis spectra of AuNPs, Au@4-MPBA and Au@4-MPBA@ β -CD NPs. Ethanol was used as the solvent for all the particle samples. **b** TEM image of Au@4-MPBA@ β -CD NPs. Scale bar is 100 nm



(18 M Ω -cm) was used for the preparation of all solutions. All glassware was cleaned by aqua regia and DI water. Soil samples containing PAHs were collected from a backyard in a residential neighborhood.

Synthesis of Au@4-MPBA@ β -CD nanoparticles

The synthesis of Au@4-MPBA@ β -CD nanoparticles (NPs) is illustrated in Scheme 1. Briefly, 625 μ L of 20 mM HAuCl₄ was diluted to 50 mL with DI water, and the solution was heated under magnetic stirring. Upon boiling, 500 μ L of 1% sodium citrate was injected rapidly into the solution and the color went from yellow to dark red then lightened to a wine red during the next 5 min of heating. The mixture was heated for another 5 min after the color change and cooled down to room temperature. The solution was centrifuged at 4200 rcf for 10 min to remove the excess sodium citrate, and citrate-stabilized AuNPs were collected and redispersed in 50 mL of DI water [24].

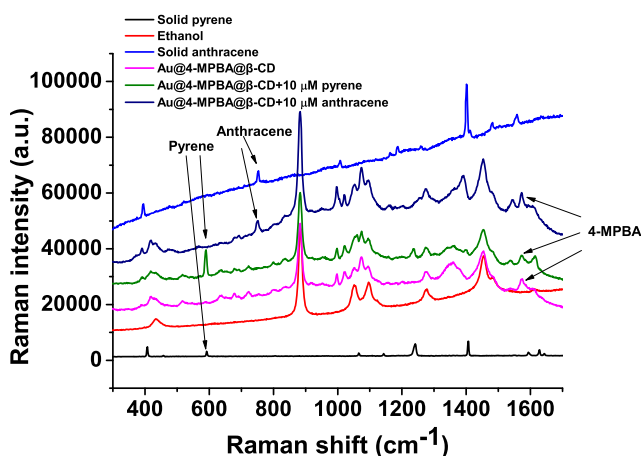


Fig. 2 Raman spectra of pyrene (solid), anthracene (solid), and ethanol. SERS spectra of Au@4-MPBA@ β -CD NP solution, 10 μ M of pyrene and anthracene mixed with of Au@4-MPBA@ β -CD NP solution, separately. Peak at 580 cm^{-1} was assigned to be pyrene peak, peak at 750 cm^{-1} to be anthracene peak and peak at 1570 cm^{-1} to be 4-MPBA peak

Five hundred μ L of 0.1 mM 4-MPBA in ethanol and water mixture solution was added into 50 mL of AuNP solution under vortex. The solution was incubated for 2 h at room temperature and centrifuged at 4200 rcf for 10 min. After removing the excess ions in the supernatant, the resulting Au@4-MPBA NPs were collected and redispersed in 50 mL of DI water [23].

In the 50 mL Au@4-MPBA NP solution, 500 μ L of 10 mM β -CD was added under sonication and vortexed. The solution was incubated overnight to form the covalent bond between boronic acid on 4-MPBA and hydroxyl group on β -CD [22]. Then, five hundred μ L of 1% sodium citrate was added under vortex and the solution was centrifuged immediately at 4200 rcf for 10 min, and excess β -CD was removed. The Au@4-MPBA@ β -CD NPs were dispersed in 5 mL of ethanol to form a concentrated nanoparticle solution.

Characterization

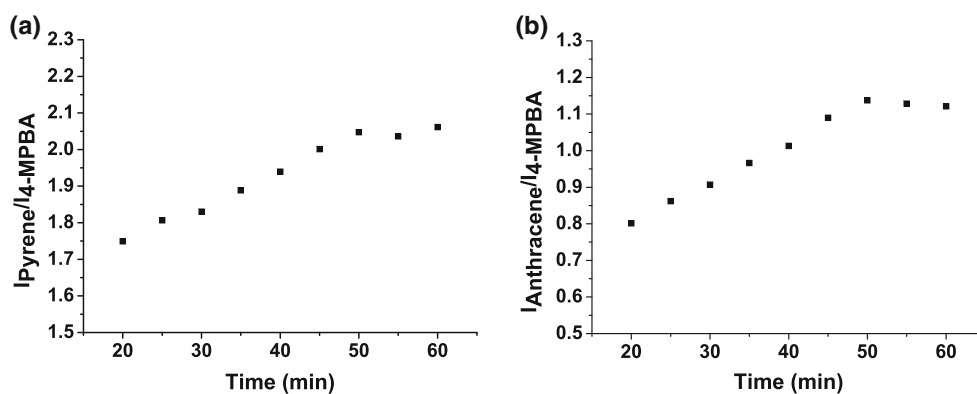
UV-vis extinction spectra of nanoparticles were measured on a USB 4000 spectrophotometer (Ocean Optics, Largo, FL). Three mL of AuNP, Au@4-MPBA NP (80 \times dilution) and Au@4-MPBA@ β -CD NP (30 \times dilution) solutions were transferred into a 1-cm path length quartz cell separately, and all measurements were performed at room temperature.

TEM images of Au@4-MPBA@ β -CD were collected on a FEI Tecnai F30 300KV transmission electron microscope. A drop of the nanoparticle solution was deposited on a formvar-covered carbon-coated copper grid from Electron Microscopy Sciences (Hatfield, PA), and dried before the imaging [25].

Raman measurement

Raman measurements were performed on a Renishaw inVia Raman microscope system. All samples involving nanoparticle solution were dispersed thoroughly in ethanol under sonication. A quartz capillary tube with a diameter of \sim 1 mm was

Fig. 3 **a** Intensity ratio of pyrene peak (580 cm^{-1}) and 4-MPBA peak (1570 cm^{-1}) against the mixing time of pyrene and Au@4-MPBA@ β -CD NPs from 20 to 60 min; **b** Intensity ratio of anthracene peak (750 cm^{-1}) and 4-MPBA peak (1570 cm^{-1}) against the mixing time of anthracene and Au@4-MPBA@ β -CD NPs from 20 to 60 min



used to hold a small amount of the sample solution, and placed on the microscope stage for Raman measurement. The microscope objective was $20\times$. A 633-nm diode laser was used in all measurements, with an intensity of 2.3 mW and exposure time of 10 s. Raman measurement of Au@4-MPBA@ β -CD NPs mixed with pyrene solutions in a capillary tube is illustrated in Scheme 2. All samples involving solid chemicals were placed on the microscope stage directly for Raman measurements. The microscope objective was $50\times$, and the measurements were done under the 633-nm diode laser with an intensity of 0.04 mW and exposure time of 10 s.

It has been reported that ethanol can enhance the SERS signal in solution [26], so all measurements of liquid samples were performed in ethanol. To identify the fingerprint peaks of 4-MPBA, pyrene and anthracene, Raman measurements of solid pyrene, solid anthracene, ethanol, Au@4-MPBA NP solution, Au@4-MPBA@ β -CD NP solution, 10 μM PAH solution (pyrene and anthracene, separately) mixed with Au@4-MPBA@ β -CD NP solution were performed.

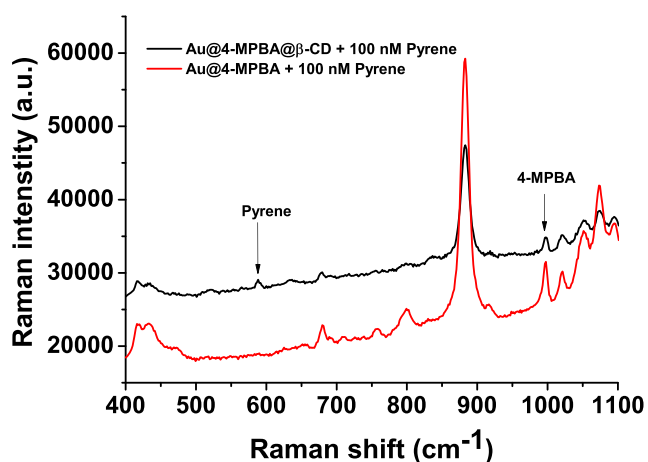


Fig. 4 SERS spectra of 100 nM pyrene mixed with Au@4-MPBA@ β -CD NPs solution and Au@4-MPBA NP solution separately. The pyrene peak at 580 cm^{-1} was observed only in the mixture with Au@4-MPBA@ β -CD NP solution

To determine the optimal mixing time, 20 μL of Au@4-MPBA@ β -CD NP solution was mixed with 40 μL of 10 μM PAH ethanol solution (pyrene and anthracene, separately), and Raman measurements were taken every 5 min from 20 to 60 min after mixing. The optimal time was chosen when the SERS signal intensity stopped increasing. To establish the relationship between the SERS signal and PAH concentration, samples with various concentrations of PAH solution (2 nM to 1 mM for pyrene solution and 10 nM to 1 mM for anthracene solution) were prepared in the same manner and Raman measurements were taken after the optimal mixing time.

PAH detection in soil samples by SERS and GC-MS

Soil samples were prepared based on the previous literature with slight modifications [27, 28]. Briefly, soil samples were crushed and sieved, then air-dried at room temperature. Approximate 0.1 g of soil sample (0.1008 g for soil sample 1 and 0.0999 g for soil sample 2) was weighed and transferred to a 20 mL glass vial separately. Two mL of acetone was added to each vial and the vials were sonicated in a water bath for 30 min. The vials were occasionally swirled to avoid soil sticking at the bottom during sonication. The extracted solutions were centrifuged at 16,800 rcf for 10 min to remove the soil. The PAH-containing supernatant was collected and acetone was dried in rotary evaporator and air. The PAHs in the vial were then dissolved in 10 mL of ethanol.

In 20 μL of Au@4-MPBA@ β -CD NP solution, 40 μL of the soil sample solution was added under sonication. The mixture was incubated for 50 min and Raman measurements were taken. Separately, the concentrations of PAHs in soil samples were independently determined by GC-MS as described in the electronic supplementary information (ESI). The experimental results were compared with those from the SERS measurements.

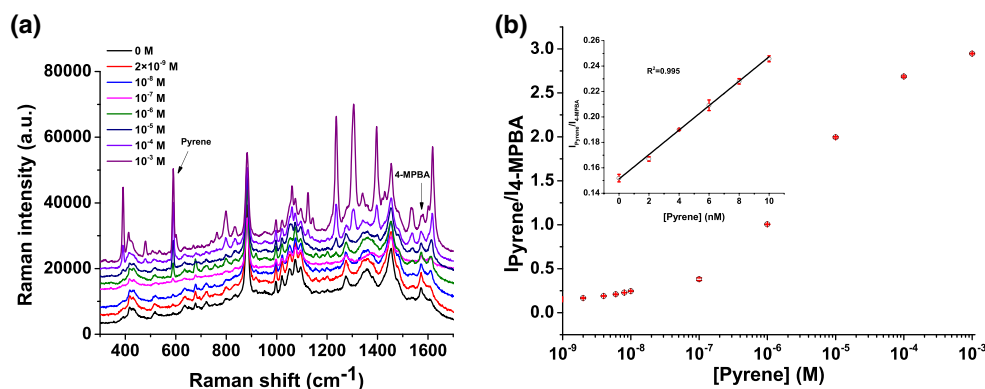


Fig. 5 **a** SERS spectra of different concentrations of pyrene (from 2×10^{-9} to 10^{-3} M, in the order from low to high) mixed with Au@4-MPBA@ β -CD NP solution. **b** Intensity ratio of pyrene peak (580 cm^{-1}) over 4-MPBA peak (1570 cm^{-1}) against pyrene concentration

(2 nM to 1 mM). Insert plot: Intensity ratio of pyrene peak (580 cm^{-1}) over 4-MPBA peak (1570 cm^{-1}) against 0, 2, 4, 6, 8 and 10 nM of pyrene. Error bars were based on three measurements at each concentration

Results and discussion

Characterization

Different concentrations of AuNP, Au@4-MPBA NP, and Au@4-MPBA@ β -CD NP solutions were characterized by UV-vis extinction spectroscopy (Fig. 1a). The band at 525 nm is the plasmon band for AuNPs. The slightly red-shifted plasmon bands (527 and 531 nm) in Au@4-MPBA NPs and Au@4-MPBA@ β -CD NPs, respectively, indicate the conjugation of 4-MPBA and β -CD to the AuNPs. No plasmon band is observed above 600 nm, suggesting the good dispersibility of the nanoparticles and no aggregation was formed. The size of the Au@4-MPBA@ β -CD NPs (~ 30 nm) was confirmed by TEM. The sizes of Au@4-MPBA@ β -CD NPs have a uniform distribution in ethanol, which were characterized by TEM and dynamic light scattering (DLS), as shown in Fig. 1b and Fig. S1. The Au@4-MPBA@ β -CD NPs were stable in ethanol for weeks.

SERS fingerprint peak and optimal mixing time determination of pyrene and anthracene

Figure 2 shows the Raman spectra of pyrene (solid), anthracene (solid), and the SERS spectra of pyrene and anthracene in Au@4-MPBA@ β -CD NP solution. According to these spectra and literature [29, 30], peak at 580 cm^{-1} is the $\nu_{\text{C-C-C}}$ mode and assigned to be pyrene peak; peak at 750 cm^{-1} is the $\nu_{\text{C-C}}$ mode and assigned to be anthracene peak; and peak at 1570 cm^{-1} is the combination of $\nu_{\text{C-C}}$ and $\beta_{\text{C-H}}$ modes and assigned to be 4-MPBA peak.

SERS measurements were taken every 5 min up to 60 min after mixing 10 μM PAHs with Au@4-MPBA@ β -CD NP solution to determine the optimal mixing time. Figure 3a and b indicate that the intensity ratio of PAHs and 4-MPBA approached constantly after 50 min. Therefore, 50 min was chosen as the optimal mixing time for all Raman measurements.

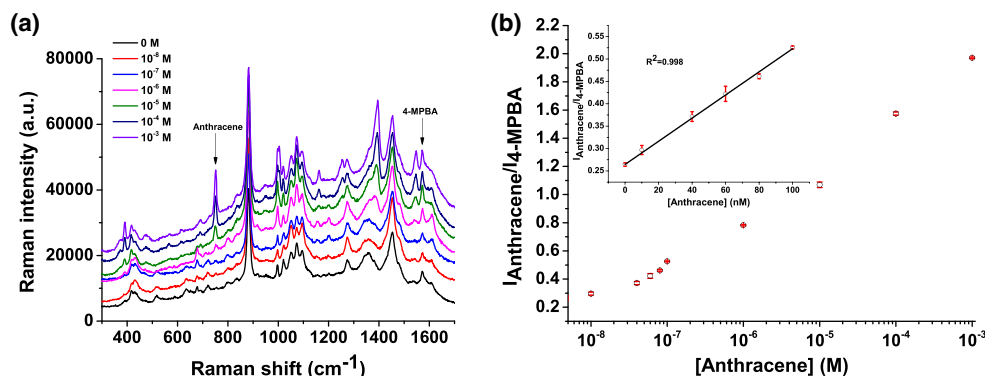


Fig. 6 **a** SERS spectra of different concentrations of anthracene (from 10^{-8} to 10^{-3} M, in the order from low to high) mixed with Au@4-MPBA@ β -CD NP solution. **b** Intensity ratio of anthracene peak (750 cm^{-1}) over 4-MPBA peak (1570 cm^{-1}) against anthracene

concentration (10 nM to 1 mM). Insert plot: Intensity ratio of anthracene peak (750 cm^{-1}) over 4-MPBA peak (1570 cm^{-1}) against 0, 10, 40, 60, 80 and 100 nM of anthracene. Error bars were based on three measurements at each concentration

Table 1 Recovery of PAHs in soil samples detected by SERS and GC-MS

	Pyrene detection			Anthracene detection		
	SERS (ng·g ⁻¹)	GC-MS (ng·g ⁻¹)	Recovery (%)	SERS (ng·g ⁻¹)	GC-MS (ng·g ⁻¹)	Recovery (%)
Sample 1	240.4 ± 1.8	236.2	101.8 ± 0.7	355.3 ± 7.8	333.8	106.4 ± 2.3
Sample 2	174.2 ± 2.4	170.0	102.5 ± 1.4	518.3 ± 7.0	509.5	101.7 ± 1.4

SERS signal enhancement of pyrene after mixing with Au@4-MPBA@β-CD NP solution

AuNPs provide rough surface and the Raman signal of 4-MPBA in Au@4-MPBA is enhanced. Yet the enhancement is insufficient to detect pyrene at low concentration with only Au@4-MPBA. With the presence of β-CD on the AuNPs surface, the Raman signals of pyrene at low concentration can be greatly enhanced. As shown in Fig. 4, when the concentration of pyrene is low, the peak at 580 cm⁻¹ is observed only in the mixture of pyrene and Au@4-MPBA@β-CD NP solution. This is most likely due to the β-CD acting as a “pocket” to bring PAH molecules close to the AuNPs surface. It has been suggested in the literature that the PAH molecule can partially fit in a β-CD “pocket”, while the exposed portion of PAH fits in another β-CD. This may allow another Au@4-MPBA@β-CD NP to approach and form a NP-PAH-NP sandwich structure [31, 32]. The hot spot between two gold nanoparticles would greatly enhance the SERS signal. In this work, the SERS signal of 100 nM pyrene is observed only through the assistance of β-CD, which is consistent with the previous literature. Thus, we demonstrate that Au@4-MPBA@β-CD NPs can be used as ultra-sensitive sensors to detect PAHs in solution.

SERS quantification of PAHs in solution

Pyrene solutions of different concentrations from 2 × 10⁻⁹ to 10⁻³ M were mixed with the same amount of Au@4-

MPBA@β-CD NP solution, and Raman measurements were carried out with results shown in Fig. 5a. The intensity of pyrene peak at 580 cm⁻¹ increases as the concentration of pyrene increases. The ratio of the peak intensity at 580 cm⁻¹ over that at 1570 cm⁻¹, $I_{\text{pyrene}}/I_{4\text{-MPBA}}$, is plotted against [pyrene], as shown in Fig. 5b. We observe a linear relationship of $I_{\text{pyrene}}/I_{4\text{-MPBA}}$ vs. [pyrene] ($R^2 = 0.995$) in the range from 2 to 10 nM, and it is used as the pyrene calibration curve. For comparison, the intensity of the peak at 580 cm⁻¹ alone, I_{pyrene} , is plotted against [pyrene], and shown in the Supplementary Information (Fig. S2), which barely displays any linear relationship. It is obvious that, with the assistance of 4-MPBA as the internal reference, quantitative determination of pyrene by SERS has become much more sensitive and reliable.

Various concentrations of anthracene solutions from 10⁻⁸ to 10⁻³ M were mixed with the same amount of Au@4-MPBA@β-CD NP solution, and Raman measurements of these mixtures were taken, as shown in Fig. 6a. The intensity of anthracene peak at 750 cm⁻¹ increases with the increase of anthracene concentration. The intensity ratio, $I_{\text{anthracene}}/I_{4\text{-MPBA}}$ is plotted against [anthracene], as shown in Fig. 6b. A linear regression with $R^2 = 0.998$ in the range from 10 to 100 nM is used as the anthracene calibration curve. Compared to the result of $I_{\text{anthracene}}$ vs. [anthracene] (Fig. S3), the SERS signals normalized by the internal reference 4-MPBA are more quantitative.

In the presence of Au@4-MPBA@β-CD NPs in solution, the pyrene concentration is quantified with a detection limit of 0.4 nM and anthracene concentration is quantified with a detection limit of 4.4 nM, based on three times the standard

Table 2 An overview on reported nanomaterial-based methods for PAH detection

Materials used	Method applied	LOD of pyrene	LOD of anthracene	Ref.
Au@4-MPBA@ β-CD NPs	SERS	0.4 × 10 ⁻⁹ M	4.4 × 10 ⁻⁹ M	This work
Fe ₃ O ₄ @Au NPs	SERS	5 × 10 ⁻⁸ M	5 × 10 ⁻⁸ M	[30]
Au NPs coupled gold film	SERS	6.3 × 10 ⁻⁸ M	–	[33]
Fe ₃ O ₄ @Ag NPs	SERS	10 ⁻⁶ M	5 × 10 ⁻⁶ M	[20]
β-CD containing polymer brush and AuNPs	SERS	8 × 10 ⁻⁹ M	2.4 × 10 ⁻⁹ M	[21]
CTAB assisted rGO-Ag NPs	SERS	10 ⁻⁶ M	–	[34]
Ag Nanorods	UTLC and SERS	10 μg·mL ⁻¹	–	[35]
Conductometric sensor	Electrochemistry	–	1.3 × 10 ⁻⁹ M	[36]

UTLC Ultra-thin layer chromatography, CTAB Hexadecyl trimethyl ammonium bromide, rGO Reduced graphene oxide

deviation above the background. The detection limit of anthracene is higher than pyrene, which is similar to what has been reported previously [21].

Detection of PAHs in soil samples

In order to evaluate the applicability and sensitivity of the method for PAHs detection in the environment, soil samples containing PAHs were analyzed by this SERS method and the conventional GC-MS method, separately. The extracted soil samples were diluted 10-fold before being measured and the SERS spectra were shown in Fig. S4. The results are summarized in Table 1. The concentrations of PAHs in the diluted soil samples were within the range of the SERS calibration curves for pyrene and anthracene, and thus, the results were calculated based on the calibration curves. The good recovery compared to the GC-MS results (Fig. S5 and Table S1) confirms that the SERS detection method with Au@4-MPBA@ β -CD NPs as SERS substrate can be used to detect PAHs at $\text{ng}\cdot\text{g}^{-1}$ (ppb) level in the original soil samples successfully. The results from this work were compared with other reported nanomaterial-based methods, which are shown in Table 2. The LOD of this method for PAHs in solution is comparable to or better than the reported methods, which indicates the sensitivity and reliability of this method.

Conclusion

We report a sensitive and less time-consuming method to detect polyaromatic hydrocarbons (pyrene and anthracene) in solution and in environmental soil samples by SERS measurement. With the conjugation of β -CD on the AuNPs, SERS signals of PAHs were enhanced and the detection limit was as low as 0.4 nM for pyrene and 4.4 nM for anthracene in solution samples. 4-MPBA was used to not only form a covalent bond with β -CD on AuNPs, but also serve as an internal reference to normalize the SERS signals for consistent and reliable measurement of the analyte. The method was applied to detect PAHs in soil samples and the results were compared to those from the conventional GC-MS measurements. The detection of pyrene in soil sample with a recovery of 101.8% and 102.5% for $236.2\text{ ng}\cdot\text{g}^{-1}$ and $170.0\text{ ng}\cdot\text{g}^{-1}$, respectively, and the detection of anthracene in soil sample with a recovery of 106.4% and 101.7% for $333.8\text{ ng}\cdot\text{g}^{-1}$ and $509.5\text{ ng}\cdot\text{g}^{-1}$, respectively, demonstrated the sensitivity and selectivity of this method in the environmental application. The Au@4-MPBA@ β -CD NP solution is straightforward to synthesize and can be stable for weeks. It is expected that this SERS method can be employed to detect other kinds of PAHs in environmental samples such as water and dust. With the development of portable Raman spectrometers, this method has great potential for field applications.

Acknowledgements Support from the Center for Environmental Genetics (CEG) of the University of Cincinnati (NIH/NIEHS grant number P30ES006096) is greatly appreciated. Z. Y. would acknowledge the Doctoral Enhancement Award from the Chemistry Department, University of Cincinnati.

Compliance with ethical standards The author(s) declare that they have no competing interests.

References

1. Laender De F, Hammer J, Hendriks AJ, Soetaert K, Janssen CR (2011) Combining monitoring data and modeling identifies PAHs as emerging contaminants in the Arctic. *Environ Sci Technol* 45: 9024–9029. <https://doi.org/10.1021/es202423f>
2. Zhang Y, Tao S (2009) Global atmospheric emission inventory of polycyclic aromatic hydrocarbons (PAHs) for 2004. *Atmos Environ* 43:812–819. <https://doi.org/10.1016/j.atmosenv.2008.10.050>
3. Rascón AJ, Azzouz A, Ballesteros E (2018) Multiresidue determination of polycyclic aromatic hydrocarbons in edible oils by liquid-liquid extraction–solid-phase extraction–gas chromatography–mass spectrometry. *Food Control* 94:268–275. <https://doi.org/10.1016/j.foodcont.2018.07.015>
4. Armstrong B, Hutchinson E, Unwin J, Fletcher T (2004) Lung cancer risk after exposure to polycyclic aromatic hydrocarbons: a review and meta-analysis. *Environ Health Perspect* 112:970–978. <https://doi.org/10.1289/ehp.6895>
5. Beyer J, Jonsson G, Porte C, Krahn MM, Ariese F (2010) Analytical methods for determining metabolites of polycyclic aromatic hydrocarbon (PAH) pollutants in fish bile: a review. *Environ Toxicol Pharmacol* 30:224–244. <https://doi.org/10.1016/j.etap.2010.08.004>
6. Diamante G, do Amaral e Silva Müller G, Menjivar-Cervantes N, Xu EG, Volz DC, Dias Bainy AC, Schlenk D (2017) Developmental toxicity of hydroxylated chrysene metabolites in zebrafish embryos. *Aquat Toxicol* 189:77–86. <https://doi.org/10.1016/j.aquatox.2017.05.013>
7. Waterman D, Horsfield B, Leistner F, Hall K, Smith S (2000) Quantification of polycyclic aromatic hydrocarbons in the NIST standard reference material (SRM1649A) urban dust using thermal desorption GC/MS. *Anal Chem* 72:3563–3567. <https://doi.org/10.1021/ac991372x>
8. De Nicola F, Concha Graña E, Aboal JR, Carballeira A, Fernandez JA, López Mahía P, Prada Rodríguez D, Muniategui Lorenzo S (2016) PAH detection in *Quercus robur* leaves and *Pinus pinaster* needles: a fast method for biomonitoring purpose. *Talanta* 153:130–137. <https://doi.org/10.1016/j.talanta.2016.01.067>
9. Poster DL, Schantz MM, Sander LC, Wise SA (2006) Analysis of polycyclic aromatic hydrocarbons (PAHs) in environmental samples: a critical review of gas chromatographic (GC) methods. *Anal Bioanal Chem* 386:859–881. <https://doi.org/10.1007/s00216-006-0771-0>
10. Taghvaei Z, Piravivanak Z, Rezaei K, Faraji M (2016) Determination of polycyclic aromatic hydrocarbons (PAHs) in olive and refined pomace olive oils with modified low temperature and ultrasound-assisted liquid–liquid extraction method followed by the HPLC/FLD. *Food Anal Methods* 9:1220–1227. <https://doi.org/10.1007/s12161-015-0297-1>
11. Gutiérrez-Valencia TM, García de Llasera MP (2017) On-line MSPD-SPE-HPLC/FLD analysis of polycyclic aromatic hydrocarbons in bovine tissues. *Food Chem* 223:82–88. <https://doi.org/10.1016/j.foodchem.2016.11.099>
12. Schmidt H, Ha NB, Pfannkuche J, Amann H, Kronfeldt HD, Kowalewska G (2004) Detection of PAHs in seawater using

- surface-enhanced Raman scattering (SERS). *Mar Pollut Bull* 49: 229–234. <https://doi.org/10.1016/j.marpolbul.2004.02.011>
13. Halvorson RA, Vikesland PJ (2010) Surface-enhanced Raman spectroscopy (SERS) for environmental analyses. *Environ Sci Technol* 44:7749–7755. <https://doi.org/10.1021/es101228z>
 14. Campion A, Kambhampati P (1988) Surface-enhanced Raman scattering. *Chem Soc Rev* 27:241–250. <https://doi.org/10.1063/1.2812122>
 15. Tang S, Li Y, Huang H, Li P, Guo Z, Luo Q, Wang Z, Chu PK, Li J, Yu XF (2017) Efficient enrichment and self-assembly of hybrid nanoparticles into removable and magnetic SERS substrates for sensitive detection of environmental pollutants. *ACS Appl Mater Interfaces* 9:7472–7480. <https://doi.org/10.1021/acsami.6b16141>
 16. Patze S, Huebner U, Liebold F, Weber K, Cialla-May D, Popp J (2017) SERS as an analytical tool in environmental science: the detection of sulfamethoxazole in the nanomolar range by applying a microfluidic cartridge setup. *Anal Chim Acta* 949:1–7. <https://doi.org/10.1016/j.aca.2016.10.009>
 17. Zhang M, Zhang X, Shi Y, Liu Z, Zhan J (2016) Surface enhanced Raman spectroscopy hyphenated with surface microextraction for in-situ detection of polycyclic aromatic hydrocarbons on food contact materials. *Talanta* 158:322–329. <https://doi.org/10.1016/j.talanta.2016.05.069>
 18. Zhong LB, Liu Q, Wu P, Niu QF, Zhang H, Zheng YM (2018) Facile on-site aqueous pollutant monitoring using a flexible, ultralight, and robust surface-enhanced Raman spectroscopy substrate: interface self-assembly of Au@Ag nanocubes on a polyvinyl chloride template. *Environ Sci Technol* 52:5812–5820. <https://doi.org/10.1021/acs.est.7b04327>
 19. Sun H, Liu H, Wu Y (2017) A green, reusable SERS film with high sensitivity for in-situ detection of thiram in apple juice. *Appl Surf Sci* 416:704–709. <https://doi.org/10.1016/j.apsusc.2017.04.159>
 20. Du J, Jing C (2011) Preparation of thiol modified Fe₃O₄@Ag magnetic SERS probe for PAHs detection and identification. *J Phys Chem C* 115:17829–17835. <https://doi.org/10.1021/jp203181c>
 21. Zengin A, Tamer U, Caykara T (2018) SERS detection of polyaromatic hydrocarbons on a β -cyclodextrin containing polymer brush. *J Raman Spectrosc* 49:452–461. <https://doi.org/10.1002/jrs.5300>
 22. Yildiz HB, Tel-Vered R, Willner I (2008) CdS nanoparticles/ β -cyclodextrin-functionalized electrodes for enhanced photoelectrochemistry. *Angew Chem Int Ed* 47:6629–6633. <https://doi.org/10.1002/anie.200801141>
 23. Yu Z, Smith ME, Zhang J, Yan J, Zhang P (2018) Determination of trichloroethylene by using self-referenced SERS and gold-core / silver-shell nanoparticles. *Microchim Acta* 185:330–336. <https://doi.org/10.1007/s00604-018-2870-y>
 24. Frens G (1973) Controlled nucleation for the regulation of the particle size in monodisperse gold suspensions. *Nat Phys Sci* 241:20–22. <https://doi.org/10.1038/physci241020a0>
 25. Zhou Y, Ding R, Joshi P, Zhang P (2015) Quantitative surface-enhanced Raman measurements with embedded internal reference. *Anal Chim Acta* 874:49–53. <https://doi.org/10.1016/j.aca.2015.03.016>
 26. Yang S, Dai X, Stogin BB, Wong TS (2016) Ultrasensitive surface-enhanced Raman scattering detection in common fluids. *Proc Natl Acad Sci* 113:268–273. <https://doi.org/10.1073/pnas.1518980113>
 27. Wang Y, Zhang J, Ding Y, Zhou J, Ni L, Sun C (2009) Quantitative determination of 16 polycyclic aromatic hydrocarbons in soil samples using solid-phase microextraction. *J Sep Sci* 32:3951–3957. <https://doi.org/10.1002/jssc.200900420>
 28. Sun F, Littlejohn D, Gibson MD (1998) Ultrasonication extraction and solid phase extraction clean-up for determination of US EPA 16 priority pollutant polycyclic aromatic hydrocarbons in soils by reversed-phase liquid chromatography with ultraviolet absorption detection. *Anal Chim Acta* 364:1–11. [https://doi.org/10.1016/S0003-2670\(98\)00186-X](https://doi.org/10.1016/S0003-2670(98)00186-X)
 29. Parlak C, Ramasami P, Tursun M, Rhyman L, Kaya MF, Atar N, Alver Ö, Senyel SM (2015) 4-Mercaptophenylboronic acid: conformation, FT-IR, Raman, OH stretching and theoretical studies. *Spectrochim Acta A Mol Biomol Spectrosc* 144:131–138. <https://doi.org/10.1016/j.saa.2015.02.040>
 30. Du J, Xu J, Sun Z, Jing C (2016) Au nanoparticles grafted on Fe₃O₄ as effective SERS substrates for label-free detection of the 16 EPA priority polycyclic aromatic hydrocarbons. *Anal Chim Acta* 915: 81–89. <https://doi.org/10.1016/j.aca.2016.02.009>
 31. Santra S, Zhang P, Tan W (1999) The restoration of pyrene fluorescence of a Cu(II)- β -cyclodextrin-pyrene. *Chem Commun* 0:1301–1302. <https://doi.org/10.1039/A903244D>
 32. Xie Y, Wang X, Han X, Song W, Ruan W, Liu J, Zhao B, Ozaki Y (2011) Selective SERS detection of each polycyclic aromatic hydrocarbon (PAH) in a mixture of five kinds of PAHs. *J Raman Spectrosc* 42:945–950. <https://doi.org/10.1002/jrs.2818>
 33. Gu HX, Hu K, Li DW, Long YT (2016) SERS detection of polycyclic aromatic hydrocarbons using a bare gold nanoparticles coupled film system. *Analyst* 141:4359–4365. <https://doi.org/10.1039/c6an00319b>
 34. Jiang M, Qian Z, Zhou X, Xin X, Wu J, Chen C, Zhang G, Xu G, Cheng Y (2014) CTAB micelles assisted rGO-AgNP hybrids for SERS detection of polycyclic aromatic hydrocarbons. *Phys Chem Chem Phys* 17:21158–21163. <https://doi.org/10.1039/c4cp04888a>
 35. Chen J, Huang YW, Zhao Y (2015) Detection of polycyclic aromatic hydrocarbons from cooking oil using ultra-thin layer chromatography and surface enhanced Raman spectroscopy. *J Mater Chem B* 3:1898–1906. <https://doi.org/10.1039/c4tb01632g>
 36. Latif U, Ping L, Dickert FL (2018) Conductometric sensor for pah detection with molecularly imprinted polymer as recognition layer. *Sensors* 18:767–775. <https://doi.org/10.3390/s18030767>

Publisher's note Springer Nature remains neutral with regard to jurisdictional claims in published maps and institutional affiliations.